J. Sleep Res. (1993) **2**, 121–129

Period-amplitude analysis and power spectral analysis: a comparison based on all-night sleep EEG recordings

BEAT A. GEERING[1], PETER ACHERMANN[1], FRITZ EGGIMANN[2] and ALEXANDER A. BORBÉLY[1]

[1] Institute of Pharmacology, University of Zürich and [2] Signal Processing Lab, Federal Institute of Technology (ETH), Zürich, Switzerland

Accepted in revised form 20 April 1993; manuscript received 14 January 1993

SUMMARY Both period-amplitude analysis (PAA) and power spectral analysis (PSA) were performed on all-night human sleep EEG recordings obtained from 11 subjects. The comparison of the two methods was based on the PAA variables *time in band* (a wave incidence measure) and *rectified amplitude*, and on the PSA variables *spectral power density* and *spectral amplitude* (the square root of power). The mean time course of these variables was determined for the first 4 nonREM–REM sleep cycles. Spectral power density and spectral amplitude in the delta range were high in nonREM sleep and low in REM sleep, and showed a declining trend over consecutive nonREM sleep episodes. In the frequency range below 2 Hz, rectified amplitude was highly correlated with both time in band and spectral amplitude, and there was no evidence for a dissociation between wave amplitude and wave incidence measures. However, in frequencies above 2 Hz, the modulation of time in band was a mirror image of that below 2 Hz. This result does not reflect a property of the data, but is inherent to the methodology applied. The reversal point of modulation was merely shifted when the high-pass filter settings were changed. It is concluded that band-pass filtering is necessary prior to PAA even for the analysis of the lowest frequency range, and that the indiscriminate use of PAA may give rise to spurious results.

KEYWORDS EEG analysis methods, Fourier analysis, period-amplitude analysis, sleep, spectral analysis, zero cross analysis

INTRODUCTION

There is an ongoing controversy on the merits of period-amplitude analysis (PAA) and power spectral analysis (PSA) in their application to the sleep EEG (e.g. Feinberg 1990a). The characteristics of the two methods are summarized in Table 1. PSA can be performed by transformation of the digitized signal into the frequency domain by the standardized Fast Fourier Transformation (FFT) procedure first published by Cooley and Tukey (1965). Adding the squared real and imaginary parts of the resulting complex values leads to the power spectrum. It is represented by a set of values in adjacent frequency bands, the resolution corresponding to the reciprocal of the duration of the transformed time epoch. The algorithm is readily available as a 'black box' procedure in numeric software library packages and in source form (e.g. Press *et al.* 1989).

PAA is computed entirely in the time domain by determining the zero voltage crossings of the digitized signal and defining the signal portions between two consecutive zero crossings as half waves. For every half wave a set of parameters can be determined, such as duration (period), amplitude, curve length and area under the curve. A rather detailed description of a PAA algorithm was published by Feinberg *et al.* (1978).

Both methods have been widely used in human and animal research and both have their advocates. Some authors prefer PSA because it provides independent measures for frequency bands and because its theoretical

Correspondence: Prof. Dr. A. A. Borbély, Institute of Pharmacology, University of Zürich, Gloriastr. 32, CH-8006 Zürich, Switzerland. Fax: +41 1 261 5684

Table 1 Characteristics of period-amplitude analysis (PAA) and power spectral analysis (PSA).

	PAA	*PSA*
elements of analysis	half waves (variable duration)	time epochs (e.g. 4 s) (constant duration)
resulting parameters	(1) number of waves (count) (2) wave duration (period) (3) wave amplitude (peak, integrated, rectified)	power spectrum (i.e., a set of frequency bins containing power values)
domain of analysis	time domain	frequency domain (after transformation from time domain)
frequency concept	instantaneous frequency: only one half wave (one frequency) at a given point in time	frequency continuum: the signal contains an infinite number of superimposed frequencies
prerequisites	no superimposed waves in signal (hardly ever fulfilled)	stationary signal within transformed epochs (not generally fulfilled)
improving measures	bandpass filtering before PAA	short epochs; average spectra over several epochs

basis is well established (for overviews see Priestley 1981; Brigham 1988; Stearns and Hush 1990). Others select PAA because of (1) its alleged ability to discriminate changes in incidence (number) from changes in amplitude of EEG waves, and (2) its intuitive grasp since it is performed in the time domain.

The advent of powerful, inexpensive computers made it possible to implement both methods in software. In the past, however, specialized devices preferentially based on zero-crossings had been used (e.g. Borbély and Neuhaus 1979).

Both methods are known to have specific limitations. Thus PAA is unable to detect fast waves riding on top of large slow waves. PSA, on the other hand, does not provide separate measures for wave amplitude and wave incidence, and it requires a stationary signal. The two methods do not appear to be equivalent in their practical application, since they do not yield concordant results. Thus on the basis of PAA, wave incidence in the theta range was decreased during recovery sleep after extended waking in humans (Feinberg *et al.* 1987) and rats (Mistlberger *et al.* 1987), whereas on the basis of PSA, theta power was increased in humans (Borbély *et al.* 1981; Dijk *et al.* 1987, 1990a) and rats (Borbély *et al.* 1984). The two methods have been reviewed by Ktonas (1987). One of his conclusions was that some of the data resulting from PAA (Bergmann *et al.* 1987; Mistlberger *et al.* 1987) "should be viewed with caution because they result from a methodology which may provide misleading information." He recommended that the EEG should be bandpass filtered in parallel for each frequency band to be analysed by PAA in order to accurately detect both slow and fast wave activity.

The interpretation of previous comparisons of PAA and PSA is difficult due to the limited datasets and some methodical problems. Thus Pigeau *et al.* (1981) who based their study on the first 25 minutes of sleep, omitted to report the high-pass filter setting and the weight vectors of their canonical correlations. Moreover, the sampling rate of 60 Hz was too low to accurately represent the signal in the time domain beyond the delta band, and the definitions of the frequency bands used in the comparison of PSA and PAA were ambiguous. In the study of Ktonas and Gosalia (1981), the lower cuttoff frequency of the polygraph amplifier (1 Hz) attenuated the signal in a major part of the frequency range investigated (0.031–2.5 Hz). Further difficulties in the interpretation of this study are caused by the different implementation of the procedures compared to many sleep studies (listed at the end of the Introduction). Thus Ktonas and Gosalia (1981) used minimum threshold criteria for analysing the amplitude and the period. This can influence the results greatly. Moreover, in their PSA implementation, the epoch length was 16 s, which was much longer than the epoch length used in most sleep studies (mostly 4 s or less, see below). Finally, to remove the DC offset, prior to the analyses they subtracted the mean value of the individual 16-s epochs from the raw data. In PAA, this procedure creates problems at the epoch transitions. An earlier comparison of PAA and PSA was restricted to the waking EEG (Beatty and Figueroa 1974).

The aim of the present study was to compare the performance of the two methods by applying them to the same dataset. We took care to use analogous procedures to those described in sufficient detail in previous sleep papers (PAA: Feinberg *et al.* 1978; Hoffmann *et al.* 1979; Bergmann *et al.* 1987; Armitage *et al.* 1989. PSA: Dumermuth *et al.* 1983; Beersma *et al.* 1990; Knowles *et al.* 1990; Åkerstedt and Kecklund 1991; Dijk *et al.* 1991).

METHODS

Subjects and data processing

Following an adaptation night, 11 healthy male subjects (mean age 25.7 y, range 23–32 y) were recorded by polysomnography for one night (8 h) in the sleep laboratory. The C3-A2 EEG derivation was amplified by a Grass 7P511 polygraph amplifier (time constant: 0.9 s). The combined action of the amplifier's 50-Hz notch filter and an analogue low pass filter served to attenuate high-frequency components (−3 dB at 27 Hz). After AD-conversion (sampling

rate 128 Hz, resolution 12 bit) and digital low-pass filtering (3 dB attenuation at 25 Hz, 24 dB/oct) the data were stored on optical disk together with the EOG and EMG.

The EEG was analysed for three high-pass filtering conditions: 0.17 Hz, 0.5 Hz, and 2.0 Hz. The time constant of the polygraph amplifier corresponded to 3 dB attenuation at a frequency of 0.17 Hz. The digitized signal was further filtered in parallel by two digital filters with cutoff slopes of 24 dB/oct, zero phase shifts, and 3 dB attenuation points at 0.5 Hz and 2.0 Hz, respectively (all digital filters: 4th order Butterworth type, Stearns and Hush 1990).

Off-line power spectral analysis (PSA) and period-amplitude analysis (PAA) were performed on the stored digitized EEG data for all three high-pass filtering conditions. To enable a strict comparison of the results, a set of 30 frequency bins was defined identically for both methods (Table 2). The bin widths were selected to provide a high resolution in the lowest delta band and in the spindle frequency range. However, to ensure an adequate representation of the waveforms in the time domain, the analyses were restricted to frequencies below 6 Hz except for the cumulative measures shown in Fig. 3. The number of samples per half wave is listed in Table 2 for all frequency bins.

Table 2 Definition of frequency bins for both PSA and PAA. The minimal half wave lengths based on a sampling frequency of 128 Hz are listed in the last column (e.g. half waves between 46.5 and 56.9 samples duration are assigned to bin 5). Note that half wave lengths are not necessarily integer values (see text). Spectral bands and half waves outside the range 0.125–25.125 Hz (512–2.5 samples per half wave) were discarded. The definition was based on the FFT epoch duration of 4 s which results in a frequency resolution of $\frac{1}{4}$ Hz.

Bin	*Width* ($\frac{1}{4}$ *Hz*)	*Low limit* (*Hz*)	*High limit* (*Hz*)	*HW-length samples*
1	1	0.125	0.375	170.7 (≤512)
2	1	0.375	0.625	102.4
3	1	0.625	0.875	73.1
4	1	0.875	1.125	56.9
5	1	1.125	1.375	46.5
6	1	1.375	1.625	39.4
7	1	1.625	1.875	34.1
8	1	1.875	2.125	30.1
9	4	2.125	3.125	20.5
10	4	3.125	4.125	15.5
11	4	4.125	5.125	12.5
12	4	5.125	6.125	10.4
13	4	6.125	7.125	9.0
14	4	7.125	8.125	7.9
15	4	8.125	9.125	7.0
16	4	9.125	10.125	6.3
17	2	10.125	10.625	6.0
18	2	10.625	11.125	5.8
19	2	11.125	11.625	5.5
20	2	11.625	12.125	5.3
21	2	12.125	12.625	5.1
22	2	12.625	13.125	4.9
23	2	13.125	13.625	4.7
24	2	13.625	14.125	4.5
25	2	14.125	14.625	4.4
26	2	14.625	15.125	4.2
27	2	15.125	15.625	4.1
28	2	15.625	16.125	4.0
29	16	16.125	20.125	3.2
30	20	20.125	25.125	2.5

Power spectral analysis

Consecutive 4-s epochs were subjected to a Fast Fourier Transformation (FFT) routine (procedure RVFFT from Mathpak87™ by Precision Plus Software, Oakville, Ontario, Canada) using a Hamming window. From the resulting complex $\frac{1}{4}$ Hz spectral bands, raw power values were computed as the sum of the squared real and imaginary parts, multiplied by the band width ($\frac{1}{4}$ Hz). After summing the raw power values into the 30 frequency bins according to Table 2, the power values were scaled to obtain μV^2. The scaling factor was defined on the basis of the total power of a 10 Hz, 50 μV (100 μV_{pp}) sine wave signal with a calculated power of 1250 μV^2. Based on visual inspection of the signal, 4-s epochs containing artifacts (2.6% of all epochs) were excluded from further analysis. The remaining 4-s spectra were averaged to yield one power spectrum per 20 s. Power *density* values can be computed by dividing power values by the respective bin width. Similar procedures have been widely used in previous studies (see Introduction for references).

Period-amplitude analysis

The portion of the EEG signal between two successive zero voltage crossings (i.e. polarity changes from positive to negative and vice versa, see Fig. 1) was considered as a half

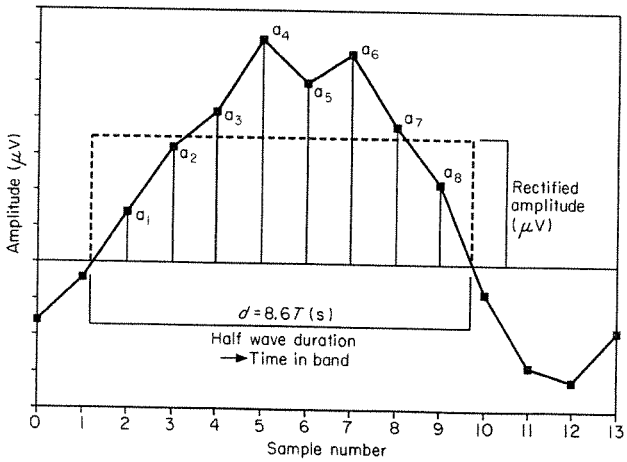

Figure 1. Period-amplitude analysis (PAA) of the digitized EEG signal. The samples of the half wave are numbered $a_1 - a_8$. The half wave duration of 8.6 samples is computed by linear interpolation at the half wave boundaries. The integrated amplitude or area under the curve is computed as $|a_1 + \cdots + a_8| \cdot T$, where T is the sampling interval. The rectified amplitude corresponds roughly to the average of all samples in the half wave and is computed by dividing integrated amplitude by time in band (d).

wave (HW). For every HW, a number of variables can be defined (Feinberg *et al.* 1978). For implementation in the present study, we selected as a wave incidence measure the HW duration (d, also expressed as the percentage of time in which the signal occupies a certain frequency band, or *% time in band*), and as a wave amplitude measure the rectified amplitude which was defined as the integrated amplitude, divided by the HW duration. The values were summed and stored for successive 20-s epochs in bins defined by the HW frequency $f = 1/(2d)$. The HW duration was defined as the time between the *interpolated* zero voltage crossings and therefore did not necessarily represent an integer multiple of the sampling interval. Half waves crossing a 20-s epoch boundary were assigned to the epoch in which they ended.

Sleep stages, sleep cycles, and data presentation

Sleep stages were visually scored for consecutive 20-s epochs according to Rechtschaffen and Kales (1968), and successive nonREM–REM sleep cycles were identified according to the criteria of Feinberg and Floyd (1979) as modified by Dijk *et al.* (1990b). All subjects completed at least 4 cycles.

To compute the average time course of the different variables over subjects, the individual nights were synchronized in the following way: in the first four sleep cycles (See Table 3 for sleep parameters) each nonREM sleep episode was subdivided into 14 equal parts (i.e. *percentiles*), and each REM sleep episode was subdivided into 3 equal parts. For each individual, average values were computed from 20-s epochs for each percentile. Epochs scored as stage 1, waking or movement time were not included in the analysis. Before averaging over subjects, the percentile values were standardized by expressing them as a percentage of the mean value of the four sleep cycles (i.e. mean of all 68 percentiles).

RESULTS

The sleep parameters for the entire bedrest episode are listed in Table 3. The average time course of spectral power density and time in band is plotted in Fig. 2. In the frequency range of 0.1–6.1 Hz spectral power density (left) shows high values in nonREM sleep and low values in REM sleep. With the exception of the 0.1–0.6 Hz bin, the peak value in nonREM sleep episode 1 exceeds the values in the subsequent episodes. The peak value in nonREM sleep episode 4 is invariably the lowest. The declining trend of power density in the low-frequency range is well documented (see Achermann and Borbély 1990 for references).

In the frequency range of 0.6–1.4 Hz, the patterns of time in band and spectral power density are similar. However, with increasing frequencies, the modulation of time in band is gradually attenuated. In frequencies higher than 2 Hz the modulation reappears and becomes progressively stronger, yet the curves are now practically mirror images of those in the low-frequency bins. Low-amplitude baseline fluctuations were responsible for the different pattern of the values in the lowest frequency bin (0.1–0.6 Hz; see end of Results section).

Wave incidence

Since the time course of the two measures of wave incidence (time in band and number of half waves) was virtually identical for the narrowly defined frequency bins ($r > 0.99$ for bins 2–30, based on 20-s values of individual nights, all

Table 3 Sleep parameters of individual subjects. All subjects were recorded for 8 hours. ID = subject number, SL = sleep latency (first occurrence of sleep stage 1), RL = REM sleep latency (from sleep onset), WASO = waking after sleep onset, MT = movement time, TST = total sleep time, SE = sleep efficiency = TST/8h, S1-S4, REMS = distribution of sleep stages (% of TST), 4CYC = total time from lights off to end of cycle 4 (only the first four cycles were used for computations). Calculations are based on 20 s epochs. Means and standard deviations are indicated in the last two rows.

ID	*SL* (*min*)	*RL* (*min*)	*WASO* (*min*)	*MT* (*min*)	*TST* (*min*)	*SE* (%)	*S1* (%)	*S2* (%)	*S3* (%)	*S4* (%)	*REMS* (%)	*4CYC* (*min*)
1	0.7	71.0	5.0	11.0	463.3	97	8	45	10	11	25	376.7
2	17.3	70.3	2.3	5.3	455.3	95	7	37	13	23	19	384.0
3	23.3	79.0	2.7	11.0	443.0	92	12	45	12	6	25	472.3
4	12.7	67.7	11.0	9.0	447.3	93	9	48	8	13	22	359.3
5	6.0	80.7	11.0	8.3	454.7	95	10	49	16	8	17	366.3
6	17.7	87.7	8.7	2.3	451.7	94	6	49	11	14	20	433.7
7	10.7	98.0	0.7	13.0	455.7	95	7	59	8	2	24	480.0
8	14.0	67.7	8.3	6.7	451.0	94	4	50	12	7	27	465.3
9	5.7	65.3	1.0	13.3	460.0	96	11	48	11	7	23	427.7
10	6.7	71.7	14.3	11.7	447.3	93	12	51	13	4	20	450.7
11	9.0	115.3	16.0	15.3	439.7	92	6	47	17	13	16	392.3
mean	11.2	79.5	7.4	9.7	451.7	94	8	48	12	10	22	418.9
s.d.	6.6	15.5	5.4	3.8	7.1	1	3	5	3	6	4	44.8

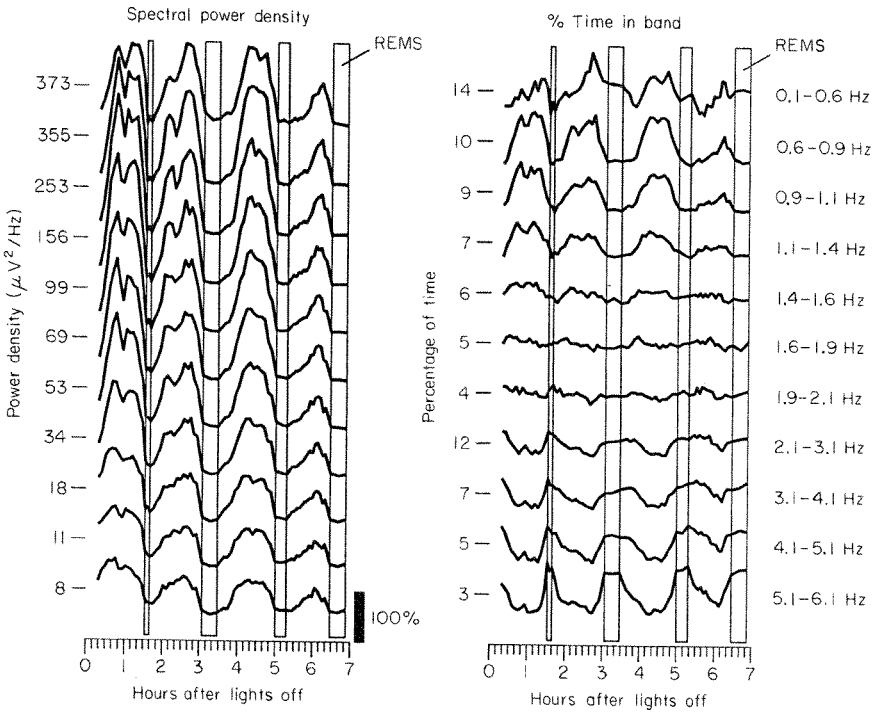

Figure 2. Comparison of the time course of spectral power density (left) and time in band (right, expressed as percentage of recording time the signal occupies a frequency band). Synchronized average curves over all subjects ($N = 11$, see text). REM sleep is delimited by vertical lines. Tick marks on the left indicate the 100% level for individual curves (common 100% calibration indicated by a black bar). Numbers on the left indicate the average values in original units corresponding to 100% (e.g. for the topmost curves, 100% corresponded to 373 μV^2/Hz for the spectral power density, and to 14% of recording time for the time in band). Frequency bands (labelled on the right for both panels) are delimited by multiples of 0.125 Hz and have been rounded to one decimal (e.g. 1.4 Hz corresponds to 1.375 Hz, see Table 2). Note the inverse relationship between the upper and lower curves for time in band, referred to in the text as 'reversal effect'.

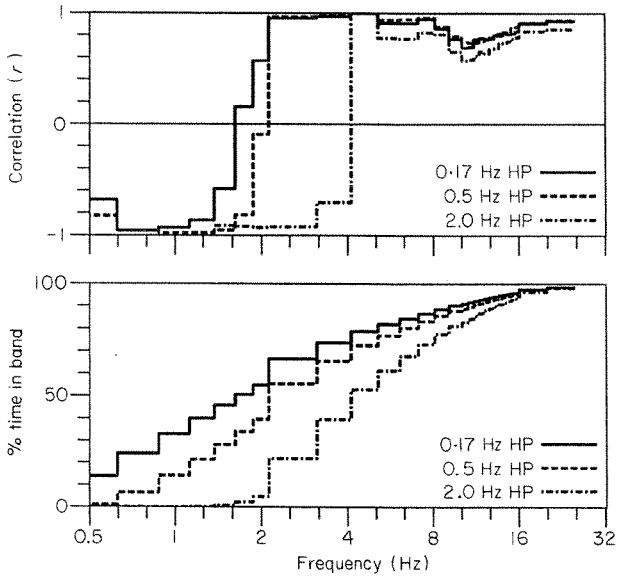

Figure 3. Effects of high-pass (HP) filtering on time in band measure. Insets indicate HP cutoff frequency. Upper panel: correlation between values in the 4.1–5.1 Hz bin (representing a higher frequency bin) and all other bins ($N = 68$, correlations computed from values averaged over 11 nights). Lower panel: cumulative time in band, i.e. percentage of time occupied by half waves up to a given frequency (mean values of pooled percentile values from 11 subjects, $N = 748$). Note the logarithmic scale of the frequency axis.

stages; $r = 0.97$ for bin 1; bins are listed in Table 2) only data for time in band are presented.

The pattern of the time in band curves (Fig. 2, right) was determined to a large extent by the values in the lowest frequencies. As has been mentioned, the curves in frequencies higher than 2 Hz were practically mirror images of those in the lowest delta band; peaks in the low frequencies corresponded to troughs in the higher frequencies. This is also evident from the high negative correlation between the values of the 0.6–0.9 Hz and 4.1–5.1 Hz bins which represent the two frequency ranges (correlation coefficient, computed for individual nights and then averaged: -0.81 ± 0.11 s.d.).

To investigate the influence of the filter setting, two further analyses were performed on the same data after digitally high-pass filtering the signal either at 0.5 Hz or at 2.0 Hz. In Fig. 3 (top) the correlation coefficients are plotted for all frequency bins versus the 4.1–5.1 Hz bin, a representative of the higher frequency range. It is evident that the different filter settings (see inset legend) did not eliminate the high negative correlation between low and high frequencies, but merely shifted the point of reversal on the frequency axis. In the original data (high-pass filter at 0.17 Hz) the reversal point was close to 2 Hz (Fig. 2). At the two higher filter settings, it was shifted towards higher frequencies.

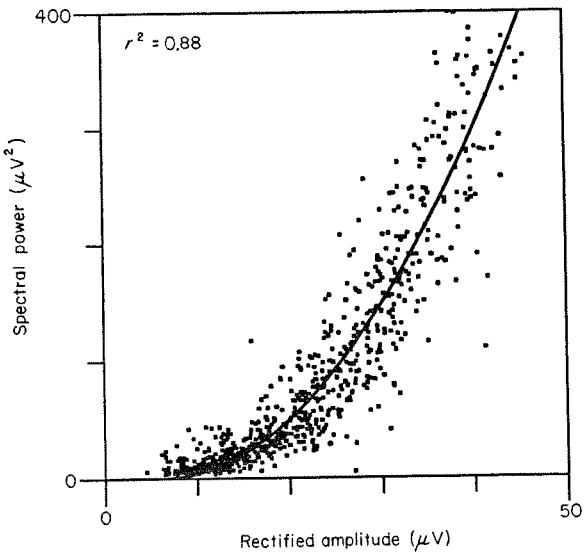

Figure 4. Relationship between rectified amplitude and spectral power computed for the 0.6–0.9 Hz bin. Percentiles were pooled from all 11 subjects ($N = 748$ data points). The parabola $(y = 0.26[x - 6.13]^2$, fitted by nonlinear regression, SAS statistical package procedure NLIN) accounted for 88% of the variance. Without the translation term (−6.13 μV) the correlation was only marginally reduced ($r^2 = 85\%$).

In all three filtering conditions a large portion of time was occupied by the slowest waves (Fig. 3, bottom; note the logarithmic frequency axis). For example in the signal filtered at 0.17 Hz, EEG half waves with a duration exceeding 0.27 seconds ($f < 1.9$ Hz) occupied about one half of an average analysis epoch (see also Fig. 2, right panel; average percentages are indicated to the left of the curves). In nonREM sleep epochs, this proportion exceeded 70%.

Amplitude

Since in theory, power is proportional to the squared signal, spectral power should exhibit a power-of-two relationship with rectified amplitude. That this was in fact the case, is evident from Fig. 4 in which a parabolic function accounted for 88% of the variance. To further compare the parameters obtained by the two methods, *spectral amplitude*, defined as the square root of spectral power, was computed for individual 20-s values obtained with the filter set at 0.17 Hz. Cumulative values were calculated over the low delta range (0.1–2.1 Hz; bins 1–8 in Table 2) for time in band, rectified amplitude and spectral amplitude. Cumulation was performed only up to 2.1 Hz to avoid the 'reversal effect' (see Fig. 2 right).

Figure 5 (left panels) shows that the time course of the three parameters was similar. High values were present in nonREM sleep and low values in REM sleep. The two amplitude-related curves corresponded even in minor details, which is also evident from their high correlation (lower scatterplot, B-A1). The correlation coefficient of the percentile data, computed for individual subjects and then averaged, was 0.98 ± 0.027 (s.d.). A high correlation was obtained also between rectified amplitude and time in band (upper scatterplot, A2–A1), although there were some differences in the time course of the two curves. During REM sleep and in the early part of nonREM sleep episodes 3 and 4, time in band was at a higher level than rectified amplitude. This means that the incidence of the waves was not reduced to the same extent as the amplitude. Conversely, in the first nonREM sleep episode, time in band was below the level of rectified amplitude. A subsequent reanalysis of the data showed that these differences vanished after digital high-pass filtering at 0.5 Hz. Moreover, the

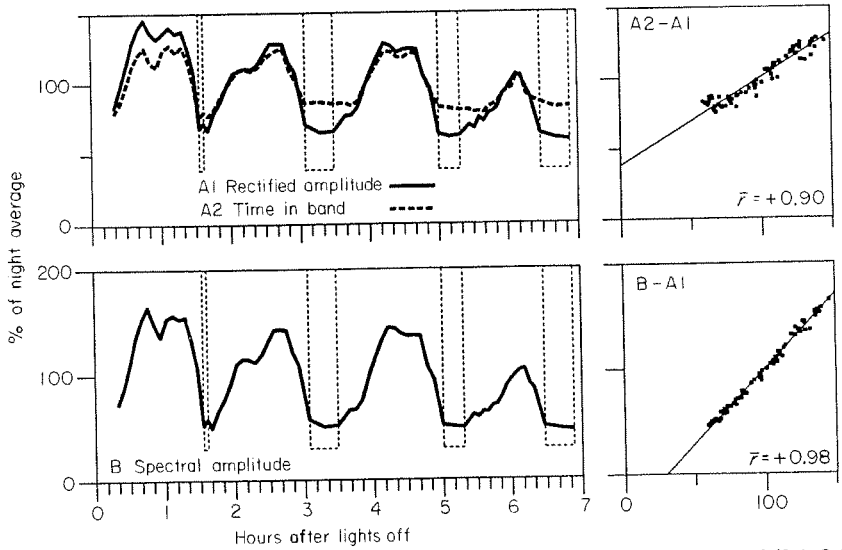

Figure 5. Comparison of variables derived from PAA (upper left) and PSA (lower left) in the low delta band (0.1–2.1 Hz). Synchronized average curves over all subjects ($N = 11$). REM sleep episodes are indicated by interrupted vertical lines. The right panels are scatterplots of pairs of the 68 average values constituting the curves in the left panels. Linear regression lines are indicated. Upper panel (A2–A1): time in band (vertical axis) *vs* rectified amplitude (horizontal axis). Lower panel (B-A1): spectral amplitude (vertical axis) *vs* rectified amplitude (horizontal axis). The indicated correlation coefficients ($\bar{r}$) are averages over 11 individual correlation coefficients ($N = 68$).

average correlation between time in band and rectified amplitude (A2–A1) increased to 0.94 ± 0.025 (s.d.), and the curve in the lowest frequency bin (Fig. 2, topmost curve of right panel) became more similar to the others (data not shown). Therefore, the differences between the two PAA measures during REM sleep were due to low-amplitude, slow baseline fluctuations (<0.5 Hz).

DISCUSSION

Problems with the wave incidence measure of PAA

In theory, PAA is capable of discriminating changes in wave incidence from changes in wave amplitude, a feature that appears to render this method superior to PSA. However, the present analysis reveals serious methodological limitations of PAA. Due to the fact that a large portion of time in band is occupied by delta waves with frequencies below 2 Hz (50% of time with a high-pass filter of 0.17 Hz; Fig. 3), the curves in the higher delta and theta bands are merely mirror images of those below 2 Hz (Fig. 2). In fact, for certain individuals the time course of the cumulated number of half waves in the delta (0.1–3.1 Hz) range showed practically no modulation over the nonREM–REM sleep cycles because the variations in the low-frequency bands were cancelled by opposite variations in the higher frequency bands. For the frequently used high-pass filter settings of 0.17 (i.e. $\frac{1}{2}$ amplitude at 0.1 Hz) and 0.5 Hz, the point of reversal was situated approximately at 2 Hz, which is surprisingly low. This means that PAA yields a reliable wave incidence measure only for the lowest delta frequencies and that data computed for the entire delta band have a strong bias towards the lowest frequency. Consequently, the finding that after sleep deprivation, wave incidence in the first nonREM sleep episode was enhanced for frequencies below 2 Hz but decreased in bands beyond 3–4 Hz (Feinberg *et al.* 1987, 1988) may have been due merely to the negative correlation of this measure in high- and low-frequency bands (see Fig. 3). An inverse relationship between wave incidence changes in high- and low-frequency bands has been also obtained in an animal study (Bergmann *et al.* 1987, Fig. 2A). To avoid spurious interpretations of the results, it is important to recognize this methodological artifact.

In the present analysis, the time course of wave incidence (i.e. time in band) and wave amplitude (i.e. rectified amplitude) in the low delta band was very similar (Fig. 5, A2 *vs* A1). This result indicates that during a normal sleep episode the two measures change in parallel and are therefore not necessarily controlled by separate biological processes. However, this conclusion is only valid when the changes are viewed on a relatively large time-scale. The two measures were found to be less concordant when they were analysed for short time intervals (Ktonas and Gosalia 1981).

Based on the report that a benzodiazepine hypnotic reduces the amplitude of delta waves while leaving their incidence unchanged (Feinberg *et al.* 1977, 1979), a superiority of PAA over PSA has been claimed. However, the basis of this conclusion is questionable since it was derived from data integrated for total sleep time which was significantly prolonged in the drug nights in comparison to baseline. When the variables were expressed per 20-s epoch, both the wave incidence (i.e. number of half waves, time in band) and the wave amplitude measures (i.e. integrated amplitude, rectified amplitude) were significantly reduced under the drug condition.

When comparing the time course of time in band and rectified amplitude (Fig. 5, top) it became evident that the wave incidence measure was markedly affected by the low-amplitude slow waves in REM sleep. The problem can be avoided by raising the cut-off frequency of the high pass filter. Nevertheless, this observation demonstrated impressively the high sensitivity of PAA to the filter setting which had been already pointed out by Gotman (1990).

Problems with high-frequency measures of PAA

It is obvious that due to the zero crossing procedure of PAA, low-amplitude fast waves riding on high-amplitude slow waves cannot be recognized. One way to overcome this limitation is to define a half wave by its peak and trough (i.e. the zero crossings of the first derivative) rather than by the zero crossings of the original signal. PAA has been complemented by this "first derivative analysis" by several authors (Hoffmann *et al.* 1979, 1984; Pigeau *et al.* 1981; Armitage *et al.* 1989, 1992; Feinberg 1990b; Uchida *et al.* 1991, 1992), although the algorithm used has not been described in detail. The first derivative is equivalent to a high-pass filter which attenuates the signal below 1/6 of the sampling frequency, and amplifies it at higher frequencies (Hamming 1989). The method therefore inevitably introduces a bias towards the fastest waves present in the signal. This is apparent in the results published by Armitage *et al.* (1992, Figs 1 + 2) in which the wave incidence measures of low and high frequencies obtained by the first derivative analysis are exactly complementary. It has been noted that the procedure is very sensitive to the presence of high-frequency noise (Frost 1987) and may even necessitate the application of a minimum amplitude criterion (Armitage *et al.* 1989). The combination of the usual PAA procedure with the first derivative analysis is not satisfactory, because neither method provides a reliable measure of intermediate frequencies, and may even yield contradictory results.

Problems with PSA

FFT routines need not to be implemented by the user, since they are readily available from software libraries (see Introduction). However, for setting up a PSA procedure, some important points should be observed (Dumermuth and Molinari 1987). To reduce *leakage* (i.e. the spreading of activity in the neighbourhood of spectral peaks), a tapered

window (reviewed by Harris 1978) should be applied. To increase the *stability* of the spectra (i.e. reduce random fluctuations), it is recommended to average power values over several epochs. Finally, the length of the transformed epochs should be short enough to ensure that the signal is approximately *stationary* within the majority of epochs. However, the lowest detectable frequency as well as the frequency resolution of the spectra are equal to the reciprocal of the epoch duration. Therefore the selection of the epoch duration represents a compromise between the contradictory requirements for stationarity and frequency resolution.

Comparison of PSA and PAA

In the low delta frequencies (<2 Hz) in which PAA yielded the most reliable measures, a very close correlation was obtained between the rectified amplitude and the spectral amplitude (i.e. the square root of spectral power; Fig. 5). Thus in the low delta range, the amplitude measures of PAA and PSA are equivalent. This is no longer necessarily the case for higher frequencies because a large part of low-amplitude waves riding upon large slow waves escape detection by PAA.

Both methods have their strong points and limitations (see Table 1). On one hand, PSA cannot discriminate wave incidence and wave amplitude, and in theory the method requires a stationary signal. Nevertheless, even if the stationarity requirement is not invariably met, PSA applied to consecutive, short (quasi-stationary) time epochs has been shown to yield functionally meaningful, quantitative measures for the sleep EEG which have been used successfully for modelling the regulation of sleep (e.g. Daan *et al.* 1984; Achermann *et al.* 1993).

On the other hand, PAA appears to be an attractive method because (1) its concept is straightforward and easy to understand and (2) it provides separate measures for the incidence and amplitude of waves. However, as the present paper demonstrates, pitfalls abound if PAA is applied to the raw EEG signal. The major problem is the dependency of measures in higher frequency bands on those in lower frequency bands. In particular, the negative correlation of the wave incidence measures may lead to misinterpretations. The 'first derivative method' does not provide a solution, but only reverses the bias. We agree therefore with the recommendation of Frost (1987) and Ktonas (1987) that PAA should be applied only to band-pass filtered signals. Signal distortion through filtering can be avoided by using digital filters with zero or linear phase-shifts (see Principe and Smith 1986a; Stearns and Hush 1990). PAA after band-pass filtering can be useful to analyse phasic events. This apparoach has been taken to recognize EEG waveforms in various frequency bands (e.g. Principe and Smith 1986b). In a similar way, Dijk *et al.* (1993) have demonstrated recently that the time course of the incidence and the amplitude of sleep spindles can differ. On the basis of the present analysis, delta wave measures in nonREM sleep are reliable for frequencies below 2 Hz. However, this limit is affected by the high-pass filter setting, and in many papers the setting has not been specified. Further difficulties may arise from the fact that in the presence of other frequency components, slow waves with a low amplitude (e.g. in REM sleep, or in nonREM sleep as a consequence of drugs or pathology) are less reliably identified by PAA than large slow waves. Therefore the requirement of band-pass filtering is also valid for the analysis of the delta frequency band.

A final comment pertains to the sampling rate. According to the Nyquist theorem the sampling rate for PSA must be at least double the highest frequency in the signal. Because PAA analyses the signal in the time domain, it requires a much higher sampling frequency (Principe and Smith 1986b). This is illustrated in Table 2 in which at a sampling rate of 128 Hz the half-waves in the highest frequency bin (24–25 Hz) are represented by only 2.5–3.2 sample points. For a broader theoretical discussion of PSA, PAA (and other EEG analysis methods), see also Lopes da Silva (1987) and Gotman (1990).

ACKNOWLEDGEMENTS

The sleep recordings used for the present analysis were obtained and scored by Daniel Aeschbach, Christian Cajochen, Sebastian Haas and Esther Werth. We thank Dr Derk-Jan Dijk and Dr Irene Tobler for their comments on the manuscript. The study was supported by the Swiss National Science Foundation, grants. nr. 31.25634.88 and 31.32574.91.

REFERENCES

Achermann, P. and Borbély, A. A. Simulation of human sleep: ultradian dynamics of electroencephalographic slow-wave activity. *J. Biol. Rhythms*, 1990, 5: 141–157.

Achermann, P., Dijk, D. J., Brunner, D. P. and Borbély, A. A. A model of human sleep homeostasis based on EEG slow-wave activity: Quantitative comparison of data and simulations. *Brain Res. Bull.*, 1993, 31: 97–113.

Åkerstedt, T. and Kecklund, G. Stability of day and night sleep—A two-year follow-up of EEG parameters in three-shift workers. *Sleep*, 1991, 14: 507–510.

Armitage, R., Hoffmann, R., Loewy, D. and Moffitt, A. Variations in period-analysed EEG asymmetry in REM and NREM sleep. *Psychophysiol.*, 1989, 26: 329–336.

Armitage, R., Roffwarg, H. P., Rush, A. J., Calhoun, J. S., Purdy, D. G. and Giles, D. E. Digital period analysis of sleep EEG in depression. *Biol. Psychiatry*, 1992, 31: 52–68.

Beatty, J. and Figueroa, C. Period analytic algorithms for the estimation of selected spectral properties of short segments of EEG data. *Behav. Res. Meth. Instrum.*, 1974, 6: 293–295.

Beersma, D. G. M., Dijk, D. J., Blok, C. G. H. and Everhardus, I. REM sleep deprivation during 5 hours leads to an immediate REM sleep rebound and to suppression of non-REM sleep intensity. *Electroenceph. Clin. Neurophysiol.*, 1990, 76: 114–122.

Bergmann, B. M., Mistlberger, R. E. and Rechtschaffen, A.

Period-amplitude analysis of rat electroencephalogram: stage and diurnal variations and effects of suprachiasmatic nuclei lesions. *Sleep,* 1987, 10: 523–536.

Borbély, A. A. and Neuhaus, H. U. Sleep-deprivation: Effects on sleep and EEG in the rat. *J. Comp. Physiol.,* 1979, 133: 71–87.

Borbély, A. A., Baumann, F., Brandeis, D., Strauch, I. and Lehmann, D. Sleep deprivation: effect on stages and EEG power density in man. *Electroenceph. Clin. Neurophysiol.,* 1981, 51: 483–493.

Borbély, A. A., Tobler, I. and Hanagasioglu, M. Effect of sleep deprivation on sleep and EEG power spectra in the rat. *Behav. Brain Res.,* 1984, 14: 171–182.

Brigham, E. O. *The Fast Fourier Transform and its Applications.* Prentice-Hall, Englewood Cliffs NJ, 1988.

Cooley, W. J. and Tukey, J. W. An algorithm for the machine calculation of complex Fourier series. *Math. Comput.,* 1965, 19: 297–301.

Daan, S., Beersma, D. G. M. and Borbély, A. A. Timing of human sleep: recovery process gated by a circadian pacemaker. *Am. J. Physiol.,* 1984, 246: R161–R178.

Dijk, D. J., Beersma, D. G. M. and Daan, S. EEG power density during nap sleep: reflection of an hourglass measuring the duration of prior wakefulness. *J. Biol. Rhythms,* 1987, 2: 207–219.

Dijk, D. J., Brunner, D. P., Beersma, D. G. M. and Borbély, A. A. Electroencephalogram power density and slow wave sleep as a function of prior waking and circadian phase. *Sleep,* 1990a, 13: 430–440.

Dijk, D. J., Brunner, D. P. and Borbély, A. A. Time course of EEG power density during long sleep in humans. *Am. J. Physiol.,* 1990b, 258: R650–R661.

Dijk, D. J., Cajochen, C., Tobler, I. and Borbély, A. A. Sleep extension in humans: sleep stages, EEG power spectra and body temperature. *Sleep,* 1991, 14: 294–306.

Dijk, D. J., Hayes, B and Czeisler, C. A. Analysis of spindle activity by transient pattern recognition software and power spectral analysis. *Sleep Res.,* 1993, 22: 426.

Dumermuth, G., Molinari, L. Spectral analysis of the EEG. *Neurophyschobiol.,* 1987, 17: 85–99.

Dumermuth, G., Lange, B., Lehmann, D., Meier, C. A., Dinkelmann, R. and Molinari, L. Spectral analysis of all-night sleep EEG in healthy adults. *Eur. Neurol.,* 1983, 22: 322–339.

Feinberg, I. How can slow wave sleep best be measured? In: M. H. Chase and T. Roth (Eds) *Slow wave sleep: its measurement and functional significance.* Brain Information Service/Brain Research Institute: UCLA, Los Angeles, 1990a: 17–20.

Feinberg, I. What is the function(s) of slow wave sleep? In: M. H. Chase and T. Roth (Eds) *Slow wave sleep: its measurement and functional significance.* Brain Information Service/Brain Research Institute: UCLA, Los Angeles, 1990b: 65–68.

Feinberg, I. and Floyd, T. C. Systematic trends across the night in human sleep cycles. *Psychophysiol.,* 1979, 16: 283–291.

Feinberg, I., Fein, G., Walker, J. M., Price, L. J., Floyd, T. C. and March, J. D. Flurazepam effects on slow-wave sleep: Stage 4 suppressed but number of delta waves constant. *Science,* 1977, 198: 847–848.

Feinberg, I., March, J. D., Fein, G., Floyd, T. C., Walker, J. M. and Price, L. Period and amplitude analysis of 0.5–3 Hz activity in NREM sleep of young adults. *Electroenceph. Clin. Neurophysiol.,* 1978, 44: 202–213.

Feinberg, I., Fein, G., Walker, J. M., Price, L. J., Floyd, T. C. and March, J. D. Flurazepam effects on sleep EEG. *Arch. Gen. Psychiat.,* 1979, 36: 95–102.

Feinberg, I., Floyd, T. C. and March, J. D. Effects of sleep loss on delta (0.3–3 Hz) EEG and eye movement density: new observations and hypotheses. *Electroenceoph. Clin. Neurophysiol.,* 1987, 67: 217–221.

Feinberg, I., Baker, T., Leder, R. and March, J. D. Response of delta (0–3 Hz) EEG and eye movement density to a night with 100 minutes of sleep. *Sleep,* 1988, 11: 473–487.

Frost, J. D., Jr. Mimetic techniques. In: A. S. Gevins and A. Rémond (Eds) *Handbook of Electroencephalography and Clinical Neurophysiology, Revised series, Vol.* 1: *Methods of analysis of brain electrical and magnetic signals.* Elsevier, Amsterdam, 1987: 195–206.

Gotman, J. The use of computers in analysis and display of EEG and evoked potentials. In: D. D. Daly and T. A. Pedley (Eds) *Current Practice of Clinical Electroencephalography.* Raven Press, New York, 1990 (2nd ed): 51–83.

Hamming, R. W. *Digital filters.* Prentice-Hall, Englewood Cliffs NJ, 1989 (3rd edn).

Harris, F. J. On the use of windows for harmonic analysis with the discrete fourier transform. *Proc. IEEE,* 1978, 66: 51–83.

Hoffmann, R., Moffitt, A., Shearer, J., Sussman, P. and Wells, R. Conceptual and methodological considerations towards the development of computer-controlled research on the electrophysiology of sleep. *Waking Sleeping,* 1979, 3: 1–16.

Hoffmann, R., Moffitt, A., Wells, R., Sussman, P., Pigeau, R. and Shearer, R. Quantitative description of sleep stage electrophysiology using digital period analytic techniques. *Sleep,* 1984, 7: 356–364.

Knowles, J. B., MacLean, A. W., Brunet, D. and Coulter, M. Nap-induced changes in the time course of process S. Effects on nocturnal slow wave activity. In: J. Horne (Ed) *Sleep* '90. Pontenagel Press, Bochum, 1990; 68–70.

Ktonas, P. Y. Editorial comment: period-amplitude EEG analysis. *Sleep,* 1987, 10: 505–507.

Ktonas, P. Y., Gosalia, A. P. Spectral analysis vs. period-amplitude analysis of narrowband EEG activity: a comparison based on the sleep delta-frequency band. *Sleep,* 1981, 4: 193–206.

Lopes da Silva, F. H. EEG analysis: theory and practice. In: E. Niedermeyer and F. H. Lopes da Silva (Eds) *Electroencephalography: basic principles, clinical applications, and related fields.* Urban & Schwarzenberg, Baltimore, 1987 (2nd edn): 871–897.

Mistlberger, R., Bergmann, B. and Rechtschaffen, A. Period-amplitude analysis of rat electroencephalogram: effects of sleep deprivation and exercise. *Sleep,* 1987, 10: 508–522.

Pigeau, R., Hoffmann, R. and Moffitt, A. A multivariate comparison between two EEG analysis techniques: Period analysis and fast Fourier Transform. *Electroenceph. Clin. Neurophysiol.,* 1981, 52: 656–658.

Press, W. H. Flaunery, B. P., Teukolsky, S. A. and Vetterling, W. T. *Numerical Recipes in Pascal: the art of scientific computing.* Cambridge University Press, Cambridge, USA, 1989 (includes floppy disks).

Priestley, M. B. *Spectral Analysis and Time Series.* Academic Press, London, 1981.

Principe, J. C. and Smith, J. R. Design and implementation of linear phase FIR filters for biological signal processing. *IEEE Trans. Biomed. Engr.,* 1986a, 33: 550–559.

Principe, J. C. and Smith, J. R. SAMICOS—a sleep analyzing microcomputer system. *IEEE Trans. Biomed. Engr.,* 1986b, 33: 935–941.

Rechtschaffen, A. and Kales, A. *A Manual of Standardized Terminology, Techniques and Scoring System for Sleep Stages of Human Subjects.* U.S. Department of Health, Education and Welfare, Public Health Service, Bethesda, MD, 1968.

Stearns, S. D. and Hush, D. R. *Digital Signal Analysis.* Prentice Hall, Englewood Cliffs, NJ, 1990 (2nd edn) (includes floppy disk).

Uchida, S., Maloney, T., March, J. D., Azari, R. and Feinberg, I. Sigma (12–15 Hz) and delta (0.3–3 Hz) EEG oscillate reciprocally within NREM sleep. *Brain Res. Bull.,* 1991, 27: 93–96.

Uchida, S., Maloney, T. and Feinberg, I. Beta (20–28 Hz) and delta (0.3–3 Hz) EEGs oscillate reciprocally across NREM and REM sleep. *Sleep,* 1992, 15: 325–358.